ELSEVIER

Journal of Crystal Growth 206 (1999) 15–22

JOURNAL OF CRYSTAL GROWTH

www.elsevier.nl/locate/jcrysgro

Structural and optical properties of 0.98 μm InGaAs/InGaAsP strained-compensated multiple quantum well structures grown by gas-source molecular beam epitaxy

Jin-Shung Liu[a], Jyh-Shyang Wang[a,*], K.Y. Hsieh[b], Hao-Hsiung Lin[a]

[a]*Department of Electrical Engineering, National Taiwan University, Room 419, Taipei, Taiwan, ROC*
[b]*Insitutes of Materials Science and Engineering, National Sun Yet-Sen University, Kaohsiung, Taiwan, ROC*

Received 2 June 1999; accepted 10 June 1999
Communicated by M. Schieber

Abstract

The effects of growth temperature on the structural and optical properties of gas-source molecular beam epitaxy grown 0.98 μm InGaAs/InGaAsP strain-compensated multiple quantum well structures were studied by transmission electron microscopy (TEM), double crystal X-ray diffraction and photoluminescence measurements. It was found that high quality of quantum well structures can be obtained at a lower growth temperature. A higher growth temperature caused an immiscible growth for the InGaAsP alloy from the observation of the TEM images. As a result, the optical and structural quality of the quantum well structure was drastically degraded.

PACS: 68.35.Ct; 68.65. + g

Keywords: Gas-source molecular beam epitaxy; Multiple quantum well; Transmission electron microscopy

1. Introduction

The Al-free InGaAs/InGaAsP/InGaP material system has increasingly become an alternate to the traditional InGaAs/GaAs/AlGaAs material system for the fabrication of 0.98 μm semiconductor lasers as the pumping source of Er^{3+}-doped 1550 nm fiber amplifiers [1–5]. The advantages of using the Al-free system for laser diodes over the Al-based system are: (1) no degradation due to oxidation of aluminum during fabrication process and laser operation is expected, (2) higher electrical [6] and thermal [7] conductivity of InGaP cladding layers results in better total power-conversion efficiencies at high power, (3) a long lifetime is expected due to the absence of dark line defects in InGa(As)P, and (4) low surface recombination [8] and less DX centers [9]. Optimization of such devices, however, requires an understanding of the nature of quantum well growth in this material system. In this respect, several related studies have been carried out for InGaAs/GaAs quantum wells in the past

* Corresponding author.
E-mail addresses: jswang@mimi.ee.ntu.edu.tw (J.-S. Wang), hhlin@mimi.ee.ntu.edu.tw (H.-H. Lin)

0022-0248/99/$ - see front matter
PII: S0022-0248(99)00317-6

years [3,10,11]. For InGaAs/InGaAsP quantum wells, the effects of substrate misorientation on the interfacial structures of metal organic chemical vapor deposition (MOCVD)-grown InGaAs/InGaAsP/InGaP quantum well laser diodes were studied by atomic force microscopy (AFM) and photoluminescence (PL) [12]. In this study, we investigated the effects of growth temperature on the structural and optical properties of InGaAs/InGaAsP quantum wells grown by gas-source molecular beam epitaxy (GSMBE) by using transmission electron microscopy (TEM), double crystal X-ray diffraction (DXRD) and PL measurements.

2. Experiments

The epitaxial growth was carried out by VG V80H GSMBE. High purity hydrides, PH_3, AsH_3, and elemental group III sources, In and Ga, were used in the GSMBE growth. PH_3 and AsH_3 were thermally decomposed to generate P_2 and As_2 in a cracker cell held at 1000°C. The cracking efficiencies were determined to be over 99% from the mass spectrometry analysis. The In and Ga fluxes were controlled by a conventional beam equivalent pressure (BEP) ratio method. The PH_3 and AsH_3 flow rates were precisely controlled by using the Baratron capacitance manometer.

0.98 μm InGaAs/InGaAsP strain-compensated multiple quantum well (MQW) structures were grown on (1 0 0)GaAs substrates at various temperatures. The designed MQW structure is a 12-period $In_{0.2}Ga_{0.8}As$ (6 nm)/$In_{0.2}Ga_{0.8}As_{0.33}P_{0.67}$ (10 nm) MQW sandwiched by two 0.2 μm-thick InGaP layers. The growth rates of InGaAs well and InGaAsP barrier were both kept at 1.3 μm/h. The V to III ratios were 3 and 6 for the growth of InGaAs wells and InGaAsP barriers, respectively. The growth temperature was varied from 430 to 520°C. In order to keep the same As composition in the InGaAsP barrier, the AsH_3 to PH_3 flow rate ratios for different growth temperatures were determined from our growth model [13,14]. After growth, the MQW structures were characterized by DXRD, TEM and PL measurements.

3. Results and discussion

3.1. Structural properties

Fig. 1 shows the (4 0 0) plane DXRD rocking curves of the MQW structures grown at 430, 460,

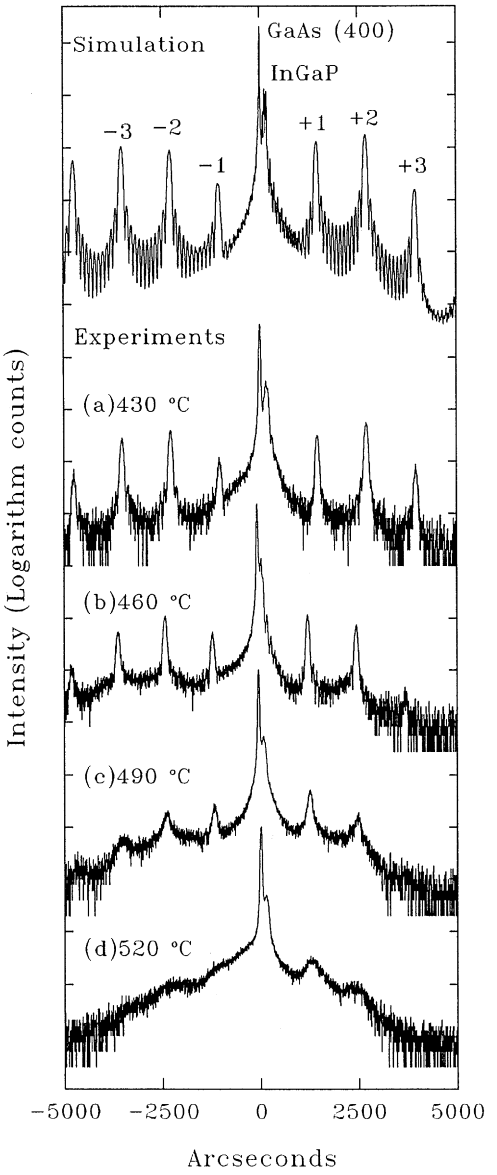

Fig. 1. The experimental (4 0 0) plane DXRD rocking curves of the InGaAs/InGaAsP SCMQW structures grown at (a) 430, (b) 460, (c) 490, and (d) 520°C, respectively, and the computer simulation curve.

490 and 520°C, respectively. The computer simulation rocking curve is also shown in the figure. Notice that the net lattice mismatches of the four samples are all less than 1×10^{-3}. The sample grown at 430°C shows strong and narrow satellite peaks. The relative intensities and full-width at half-maximum (FWHMs) of the satellite peaks are all in excellent agreement with those of the simulation curve. This indicates that the individual layers are of good crystal structure and the interfaces between the layers are very sharp. The rocking curve of the sample grown at 460°C also shows narrow and well-defined satellite peaks. The relative intensity is also close to the simulation curve. The overall peak intensity is only slightly smaller than that of the sample grown at 430°C. However, as the temperature increases to 490 and 520°C, higher order of satellite peaks disappear and lower order of peaks become weaker and broader. This reveals that the crystal structures and the interface abruptness of the MQWs have been seriously degraded.

The degradation in structural quality at higher growth temperatures can be observed more clearly from their TEM images. Figs. 2a–d show the dark-field (0 1 1) and (0 $\bar{1}$ 1) cross-sectional TEM images with the diffraction vector $g = (2\,0\,0)$ for samples grown at 430, 460, 490 and 520°C, respectively. The sample grown at 430°C has flat interfaces between the barriers and wells throughout the structure when viewed from the (0 1 1) cross section. Alternatively, the interfaces are slightly less flat but still of

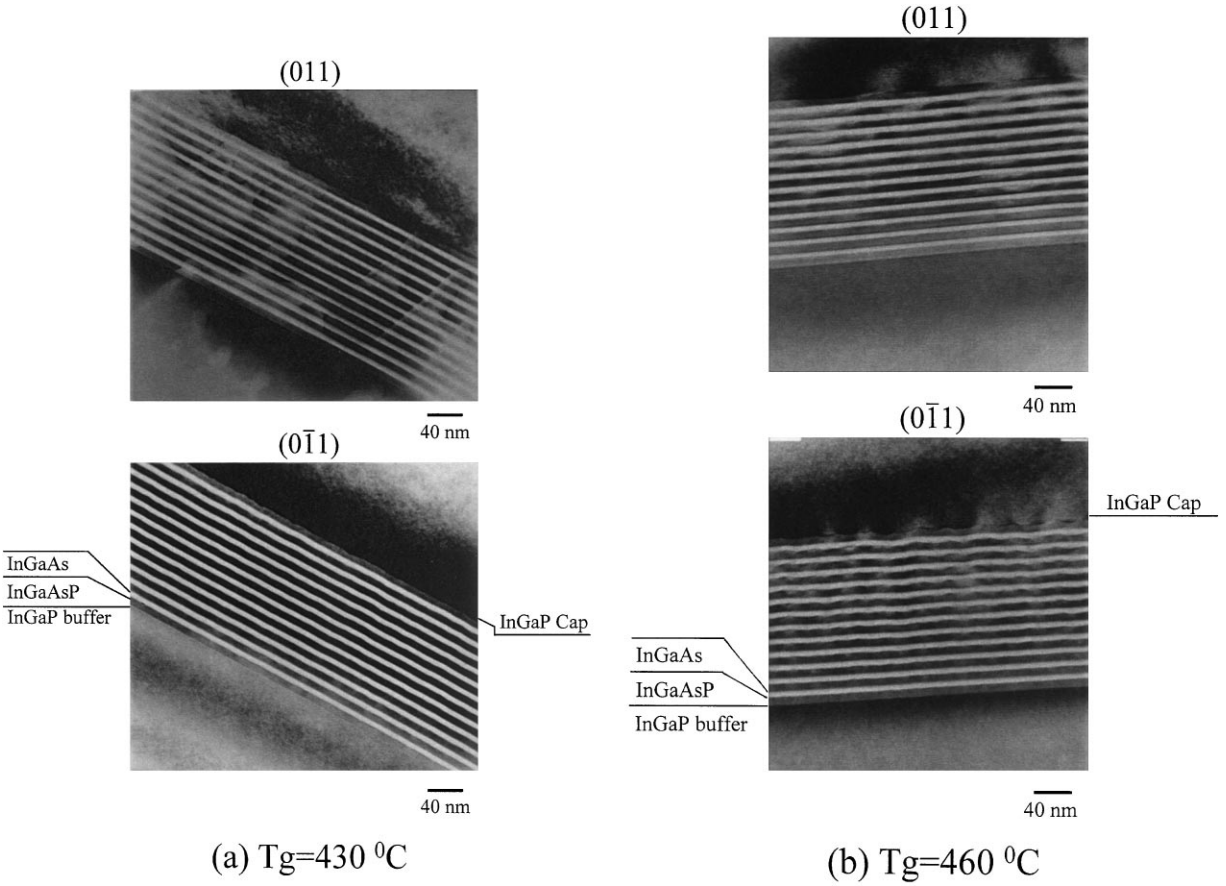

Fig. 2. The dark-field (0 1 1) and (0 $\bar{1}$ 1) cross-sectional TEM images with the diffraction vector $g = (2\,0\,0)$ for the InGaAs/InGaAsP SCMQW structures grown at (a) 430, (b) 460, (c) 490 and (d) 520°C, respectively.

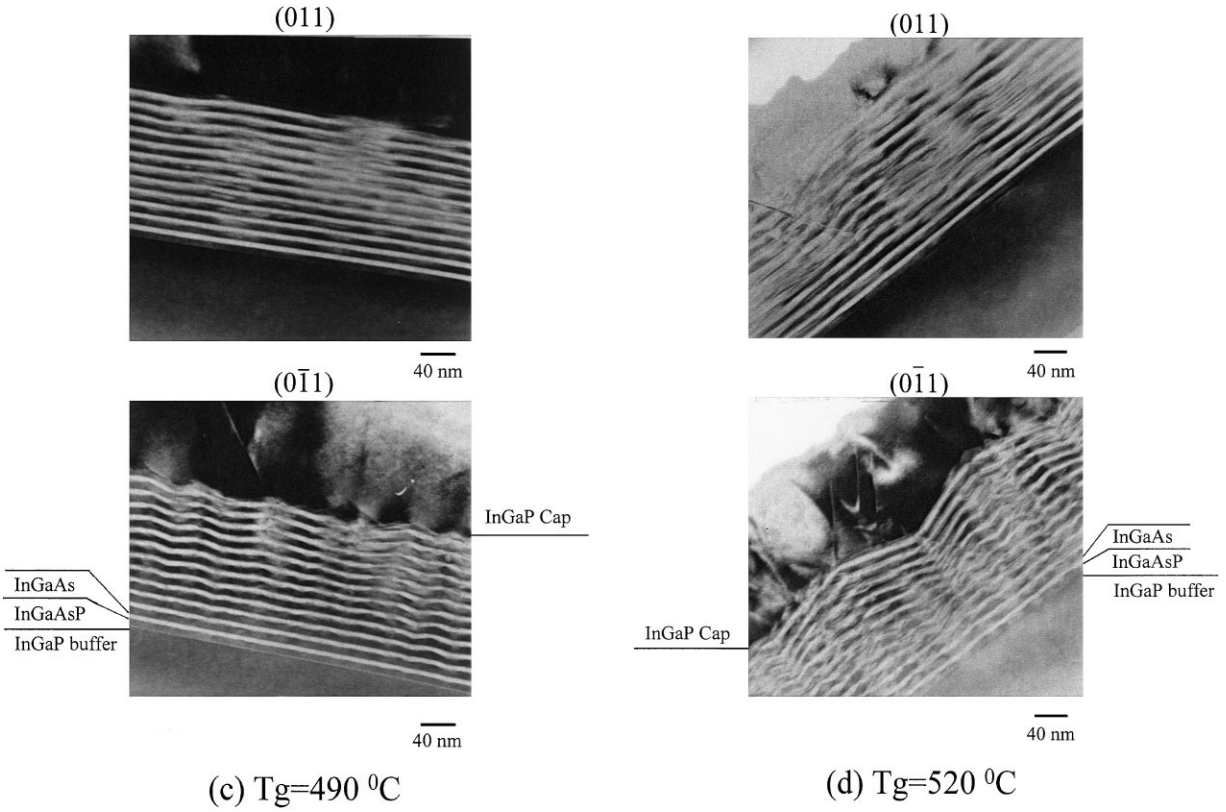

Fig. 2. *Continued.*

reasonably good quality when viewed from the (0 $\bar{1}$ 1) cross section. The sample grown at 460°C also shows similar interface flatness in the (0 1 1) cross section. However, when viewed from the (0 $\bar{1}$ 1) cross section, the interfaces are obviously degraded. It can be seen that they are not planar and present undulations along the [0 1 1] direction. The undulation occurred mainly in the interfaces from the InGaAsP barriers to the InGaAs wells and became more drastic with the increase of the grown periods of quantum wells. Alternatively, the interfaces from the InGaAs wells to the InGaAsP barriers are less undulated and have less change in their flatness with the increase of the grown periods of quantum wells. Therefore, it seems that the growth of the InGaAsP barriers at this temperature had tended to become three-dimensional (3D) island growth and roughened the growth surface but those of the InGaAs well tended to still maintain as two-dimensional (2D) growth mode and restored the flatness of the surfaces. On the other hand, it can be found that there exist strong contrast modulations along the [0 1 1] direction inside the InGaAsP layers. The contrast modulations may be due to the lateral modulations of the composition, strain or thickness. However, because of no obvious contrast modulations inside the InGaAs wells where there are also the same degrees of thickness modulations, the lateral composition and strain modulations are the main causes for the observed contrast modulations inside the InGaAsP barriers. Finally, a noticeable feature is that there are strong contrasts between the top InGaAsP barrier and the InGaP cap layer around the maximum of the undulations. This reveals that there are large strains distributed in those regions [15].

For the samples grown at 490 and 520°C, the interface quality in the (0 1 1) cross sections also

become degraded. On the other hand, the overall quantum well structures in the (0 $\bar{1}$ 1) cross sections have been seriously degraded. For the first three periods of quantum wells, it can be seen that although the interfaces from InGaAs to InGaAsP are maintained as similarly flat as those of the sample grown at 460°C, the undulations of the interfaces from InGaAsP to InGaAs become more drastic and the contrast modulations inside the InGaAsP barriers also become stronger. The oscillation amplitude of the undulation also increases with the periods of quantum wells. In addition, it can be found that its relative position is maintained from one InGaAsP barrier to another although the InGaAs wells between the barriers have restored the surfaces in almost same flatness. This causes the formation of columnar structures lining up quasiperiodically in the [0 1 1] direction and with a period length of about 20–30 nm. In fact, these phenomena can be also found for the sample grown at 460°C but are more blurred. The columnar structures begin to merge with each other after the fourth quantum well. This not only results in stronger undulations in the InGaAsP barriers but also causes that the following grown InGaAs well cannot restore the flatness of the surface. As a result, undulations also occur in the InGaAs wells. Such a behavior that the columnar structures merges with each other occurs again and again and eventually results in triangle-shaped structures with the oscillation amplitude as large as 30 nm and the period as long as 200 nm for the sample grown at 520°C. In addition, it can be seen that there are dislocations generated from the top InGaAsP barrier and extended to the InGaP cap layer in these two samples. This reveals that the accumulated strain energies there have become high enough to cause the lattice relaxation and the occurrence of dislocations.

Based on the above observations, the origin and the process for the degradation of the MQW structures are as follows. First, the TEM images reveal that higher growth temperatures caused the composition modulations along the [0 1 1] direction inside the tensile-strained InGaAsP layers. This phenomenon had already begun occurring once the growth was switched from the InGaP buffer layer to the first InGaAsP layer. Such composition modulations caused some regions with larger tensile strains and some other regions with smaller tensile strains in the InGaAsP layers. According to the thermodynamic analysis [16], once a composition modulation is initiated, it will assume a periodic form and propagate as the epilayer growth proceeds. In this way, the thickness of InGaAsP in the region with a larger tensile strain would eventually become larger than its critical thickness for a two-dimensional (2D) growth. As a result, a 3D island growth similar to the Stranski–Krastanov (SK)-mode growth was initialized to relax the large surface strain [17]. That is, although the average strains of the InGaAsP layers grown at different temperatures are of about the same values and are all small enough to avoid strain-induced island growth, the local large strains occurring in the InGaAsP layers grown at higher temperatures due to composition modulations are still possibly to make the strain-induced island growth occur earlier. Alternatively, there was no composition modulation occurring inside the InGaAs compressive-strained layer from the observation of their TEM images. Therefore, there would be no local regions with strains high enough to induce island growth for the InGaAs layers. As a result, the InGaAs layers were still maintained as 2D growth and restored the flatness of the surfaces.

On the other hand, the large tensile strain around the island regions of the first InGaAsP layer would induce larger compressive stresses on the following overgrown InGaAs layer. Therefore, when the second tensile-strained InGaAsP layer was being grown on, InGaAsP with larger tensile strains after the composition modulations would be deposited on InGaAs overgrown around the islands to obtain smaller lattice-mismatches and reduce the strain energies. As a result, the same kind of composition modulations propagated and the relative positions of the island regions were maintained from those of the first InGaAsP layer. In addition, the tensile strains around the island regions of the first InGaAsP layer would be too large to be completely compensated by the compressive strains of the overgrown InGaAs. The residual tensile-strains would then cause larger tensile-strains accumulated in the next InGaAsP layer and make the island growth of the second InGaAsP layer

occur earlier. These descriptions explain why the relative position of undulation in the second InGaAsP barrier was maintained from that of the first InGaAsP barrier and its oscillation amplitude became more drastic although the surface of the first InGaAs well had been recovered to be flat. The columnar structures were then formed as such a process was continued. In fact, such a formation mechanism of the columnar structure is similar to that of the self-organized InAs/GaAs quantum dots structures and devices where using multiple periods of InAs/GaAs to form vertically aligned quantum-dot stacks and larger size of quantum dots [18]. Pearsh et al. had also used the similar mechanism to grow multiple quantum wires [19].

On the other hand, as the sizes of the islands became too large, they merged with each other and formed larger islands. This resulted in the overall quantum well structure to be transfigured. Eventually, the strains around the island regions became too large and resulted in the lattice relaxation and the occurrence of dislocation. The quantum well structures were then entirely seriously degraded.

With regard to the origins of the composition modulations in the InGaAsP layers grown at higher temperatures, the most possible reason is due to the occurrence of the so-called spinodal-like decomposition in these layers. According to the thermodynamic calculation [20], the composition of this InGaAsP lies within the spinodal isotherm for the growth temperature of 550°C. That is, for a growth temperature below 550°C, this alloy is energetically unstable and any composition fluctuation will decrease the Gibbs free energy, and as a result, it will undergo phase separation. Such phenomena have been observed for the InGaAsP grown on InP by GSMBE [21–23]. To avoid such an immiscible growth, a sufficiently high growth temperature is required for LPE and MOCVD growth to make the alloy composition lie outside the spinodal isotherm [2,24]. However, for MBE growth, it appears that kinetic limitations, whereby the surface adatom diffusion lengths are reduced via a lower growth temperature in association with a higher V/III and higher growth rate, limit the ability of the system to achieve equilibrium resulting less decomposition. This explains why high quality of quantum well structures were obtained at lower growth temperatures in our experiments. It is worthy to notice that the strain-induced island growth will also proceed more quickly with the increase of growth temperature. This will also cause the quantum well structure grown at higher temperatures to be degraded more drastically. On the other hand, when the phase separation occurs, there will be more stronger modulations of composition and thickness along the [0 1 1] direction as the diffusion length along [0 1 1] direction is larger than that along [0 $\bar{1}$ 1] direction for adatoms on the (1 0 0) growth surface [21]. This explains why the degradation of the quantum well structure is anisotropic.

3.2. Optical properties

The quality degradation at higher growth temperatures was also found in the PL measurements. Fig. 3 shows the room-temperature PL spectra of these MQW structures. The FWHM of the peak is as narrow as 40 meV for the sample grown at 430°C. This confirms again the high quality of this sample. When the growth temperature increases, it can also be seen that the peak becomes broaden.

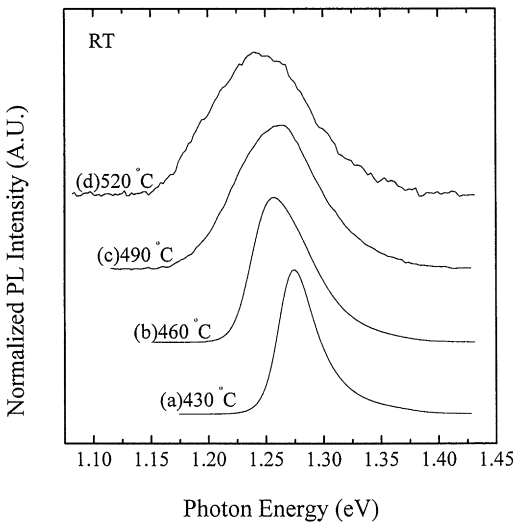

Fig. 3. The RT PL spectra of the InGaAs/InGaAsP SCMQW structures grown at (a) 430, (b) 460, (c) 490, and (d) 520°C, respectively.

Fig. 4 shows the peak intensity and FWHM as a function of the growth temperature. The intensity and FWHM are kept about the same for the growth temperature lower than 450°C. However, as the growth temperature is higher than 460°C, the intensity and FWHM are drastically degraded. The decrease in the peak intensity is as large as three-orders of magnitude and the broadening in the peak FWHM is as large as three-fold when the growth temperature increases to 520°C. Fig. 5 shows the 8.5 K PL spectra of these MQW structures. Only an emission peak with its FWHM as narrow as 18 meV can be found for the sample grown at 430°C. However, an additional strong emission peak appearing in lower-energy side was found when the growth temperature is higher than 460°C. Its peak position shifts to a lower energy with the increase of growth temperature. Such PL features just result from the more drastic composition modulations and thickness fluctuations in the quantum wells as the growth temperatures increases.

4. Conclusions

In conclusion, we have grown a series of 0.98 μm InGaAs/InGaAsP strain-compensation multiple quantum well structures by gas-source molecular beam epitaxy. The effects of growth temperature on both the structural and optical properties of the quantum well structures were investigated. It was found that high quality of quantum well structures can be obtained at a lower growth temperature. A higher growth temperature caused an immiscible growth for the InGaAsP alloy from the observation of the transmission electron microscopy images. As a result, the optical and structural quality of the quantum well structure were drastically degraded.

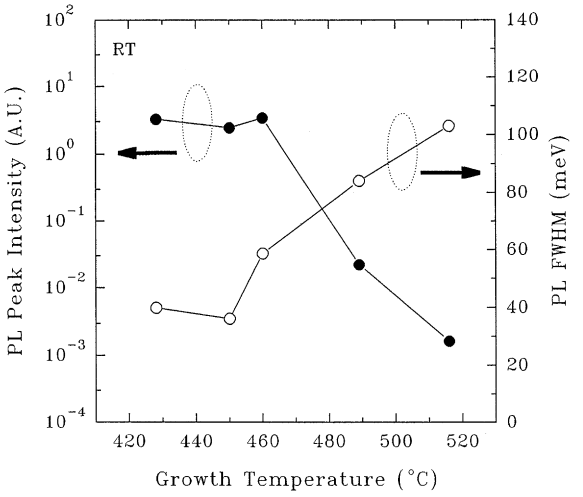

Fig. 4. The RT PL peak intensity and FWHM as a function of growth temperature for the InGaAs/InGaAsP SCMQW structures.

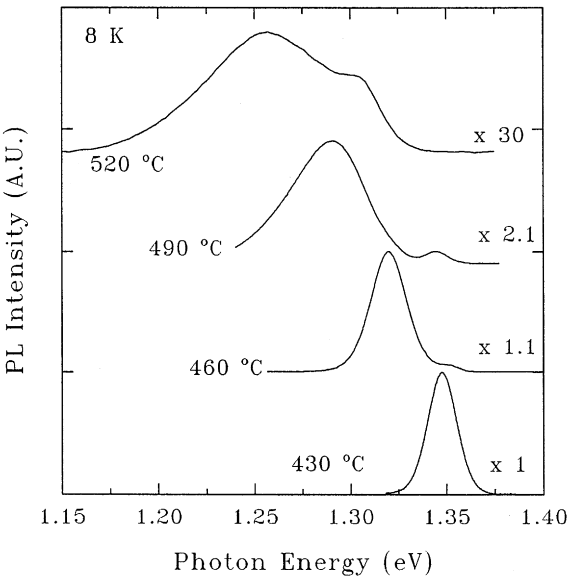

Fig. 5. The 8.5 K PL spectra of the InGaAs/InGaAsP SCMQW structures grown at (a) 430, (b) 460, (c) 490, and (d) 520°C, respectively.

Acknowledgements

This work was supported by the National Science Council, ROC (NSC 87-2215-E-002-010).

References

[1] P. Savolainen, M. Toivonen, H. Asonen, M. Pessa, R. Murison Ohkubo, T. Ijichi, A. Iketani, T. Kikuta, IEEE Photon. Technol. Lett. 8 (1996) 986.
[2] M. Ohkubo, T. Ijichi, A. Iketani, T. Kikuta, IEEE J. Quantum Electron. 30 (1994) 408.

[3] G. Zhang, A. Ovtchinnikov, J. Nappi, H. Asonen, M. Pessa, IEEE J. Quantum Electron. 29 (1993) 1943.
[4] E.C. Vail, R.F. Nabiev, C.J. Chang-Hasnain, IEEE Photon. Technol. Lett. 6 (1994) 1303.
[5] P. Savolainen, M. Toivonen, H. Asonen, M. Pessa, R. Murison, IEEE Photon. Technol. Lett. 8 (1996) 986.
[6] J. Diaz, I. Eliashevich, K. Mobarhan, E. Kolev, L.J. Wang, D. Garbuzov, M. Razeghi, IEEE Photon. Technol. Lett. 6 (1994) 132.
[7] W. Nakwaski, J. Appl. Phys. 64 (1988) 159.
[8] J.M. Olson, R.K. Ahrenkiel, D.J. Dunlavy, B. Keyes, A.E. Kibbler, Appl. Phys. Lett. 55 (1989) 1208.
[9] F. Omnes, M. Razeghi, Appl. Phys. Lett. 59 (1991) 1034.
[10] K. Hiramoto, T. Tsuchiya, M. Sagawa, K. Uomoi, J. Crystal Growth 145 (1994) 133.
[11] G.P. Kothiyal, P. Bhattacharya, J. Appl. Phys. 63 (1988) 133.
[12] A. Bhattacharya, L.J. Mawst, S. Nayak, J. Li, T.F. Kuech, Appl. Phys. Lett. 68 (1996) 2240.
[13] J.S. Liu, T.L. Lee, H.H. Lin, Opt. Quantum Electron. 28 (1996) 1296.
[14] J.S. Liu, T.L. Lee, H.H. Lin, Proceedings of Eighth International Conference on Indium Phosphide and Related Materials, Schwäbisch Gmünd, Germany, 1996, p. 533.
[15] A. Ponchet, A. Rocher, J.Y. Emery, C. Starck, L. Goldstein, J. Appl. Phys. 74 (1993) 3778.
[16] F. Glass, J. Appl. Phys. 62 (1987) 3201.
[17] E. Tournie, K. Ploog, J. Crystal Growth 135 (1994) 97.
[18] Q. Xie, A. Madhukar, P. Chen, N.P. Kobayashi, Phys. Rev. Lett. 75 (1995) 2542.
[19] P.J. Pearah, A.C. Chen, A.M. Moy, K.C. Hsieh, K.Y. Cheng, IEEE J. Quantum Electron. 30 (1994) 608.
[20] K. Onabe, Jpn. J. Appl. Phys. 22 (1983) 663.
[21] R.R. Lapierre, T. Okada, B.J. Robinson, D.A. Thompson, G.C. Weatherly, J. Crystal Growth 155 (1995) 1.
[22] J.Y. Emery, C. Starck, L. Goldstein, A. Ponchet, A. Rocher, J. Crystal Growth 127 (1993) 241.
[23] K. Tappura, J. Laurila, J. Crystal Growth 131 (1993) 309.
[24] S. Mukai, J. Appl. Phys. 54 (1983) 2635.